DESIGN AND FABRICATION OF PIEZOELECTRIC ALUMINUM NITRIDE CORRUGATED BEAM ENERGY HARVESTER

Taku Hirasawa[1], Ting-Ta Yen[1*], Paul K. Wright[1], Albert P. Pisano[1], and Liwei Lin[1]
[1]Berkeley Sensor and Actuator Center, University of California at Berkeley, CA, USA
*Presenting Author: Ting-Ta Yen, ttyen@eecs.berkeley.edu

Abstract: An aluminum nitride (AlN) corrugated beam structure for MEMS energy harvester applications has been studied and demonstrated. The corrugated design in the cross section of the structure prevents the cancellation of piezoelectric effects and maintains the simple beam fabrication process with only a single deposition of piezoelectric layer. With the optimized corrugation design, this corrugated beam energy harvester can achieve the same or higher energy conversion efficiency compared with a bimorph structure. A prototype device resonating at 853Hz with output power of 0.18μW at 1G acceleration was recorded.

Keywords: vibration energy harvester, corrugation, piezoelectric, aluminum nitride (AlN), conversion efficiency

INTRODUCTION

Energy conversion efficiency is an important parameter for the design of energy harvester. Low conversion efficiency results in large device size to generate necessary output power. In general, the conversion efficiencies of piezoelectric materials are higher than those of electrostatic or electromagnetic materials[1] such that energy harvesters based on piezoelectric effect have attracted great research interests[2-5]. In order to prevent the cancellation of the generated electric fields in the piezoelectric layer, unimorph structures consisting of a single piezoelectric layer and an inactive base layer have been widely adapted in many conventional energy harvesters due to the simple fabrication process. However, the strain energy in the base layer of the unimorph structure could not be converted into electrical energy and it is therefore not efficient when compared with the bimorph structure. On the other hand, bimorph structures consisting of two piezoelectric layers have been used in bulk vibration energy harvesters but have not been commonly adapted in MEMS structures. One reason is the difficulty in piling up good piezoelectric thin films and to control the direction of polarization.

This work proposes aluminum nitride (AlN) corrugated piezoelectric beam structures utilizing the combined advantages of unimorph and bimorph structures in terms of simple process and higher energy conversion efficiency, respectively. Fabrication and experiments of prototype devices are characterized to validate the corrugated design concept.

CONCEPT AND ANALYSIS

Figure 1 shows the schematic drawing of the proposed structure based on silicon micromachining. It consists of a proof mass, corrugated supporting beam structure, and electrodes. Instead of unimorph or bimorph designs, the cross section of the piezoelectric beam has corrugated design as illustrated in Fig. 2. The total volume of the upper half corrugation is designed to be the same as the lower half such that the neutral plane remains at the center plane of the beam. When a bending force is applied, the direction of the generated electric field above the neutral plane is opposite to that beneath it. The electric power can be extracted out from both the upper and lower parts of the single corrugated piezoelectric layer from separated electrodes independently without encountering the cancellation effect in the unimorph design.

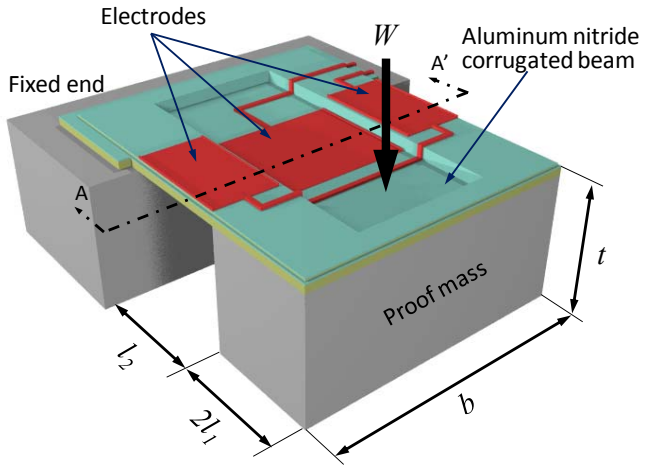

Fig. 1 Concept drawing of a piezoelectric energy harvester consisting of a cantilever supporting beam structure with corrugated cross section.

The corrugated design is reconfigurable as the resonance frequency, size of cantilever, and weight of the proof mass can be adjusted depending on the specific vibration sources and applications. Therefore, it is important to optimize the structural design to achieve high energy conversion efficiency. As illustrated in Fig. 1, the beam length and width are defined as l_2 and b respectively. Proof mass can be modeled as a static force, W, which is applied at a distance l_1 away from the tip of the beam. Unlike the moment of inertia of unimorph or bimorph beams which can only be adjusted by changing the thickness of the beam, the moment of inertia of a corrugated beam can be easily adjusted by changing the corrugation depth.

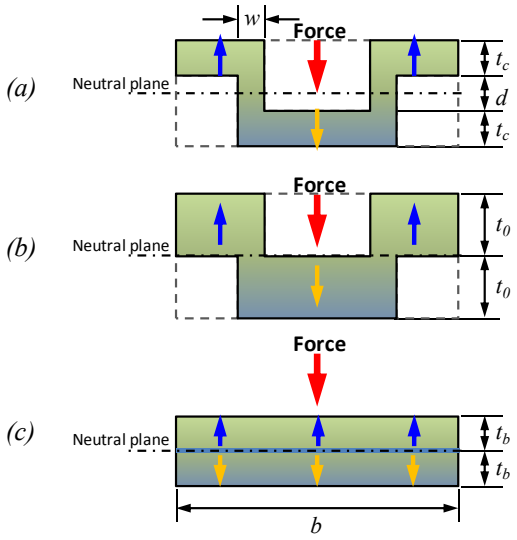

Fig. 2 Cross sections of different piezoelectric beam designs where the generated electric fields above and beneath the neutral plane are opposite in directions: (a) and (b) Two corrugated cross section designs; (c) A bimorph structure.

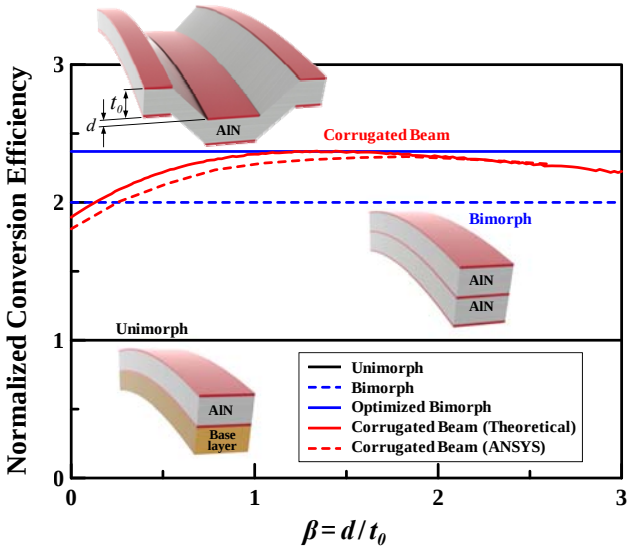

Fig. 3 Normalized conversion efficiency versus corrugation, β, which is defined as the ratio of the distance between upper and lower parts against the initial thickness.

The schematic drawings of the cross section along AA' is illustrated in Fig. 2 where d is the distance between the upper and the lower parts, t_c is the thickness of the piezoelectric layer (Fig. 2(a)), t_0 is the initial thickness of piezoelectric layer when the distance d is zero (Fig. 2(b)), and t_b is the thickness of a single piezoelectric layer in a bimorph structure (Fig. 2(c)). The stiffness of the connecting parts between the upper and lower piezoelectric layer also plays an important role and they are modeled as vertical walls with width w as shown in Fig. 2(a). The basic assumption in the analyses is that these different designs should operate under the same environmental vibration frequency. Therefore, the moment of inertia of these different structures must be the same to excite the same resonance frequency. The dimensions of corrugated beam should therefore satisfy Eq. 1:

$$4\alpha^3 + 6\alpha^2\beta + 3\alpha\beta^2 + \gamma\ \beta^3 = 4 \qquad (1)$$

where α, β, and γ are the ratio of t_c, d, and w to t_0 respectably and the relationship between t_0 and t_b is therefore defined.

Next we compared the conversion efficiency of the corrugated beam, bimorph, and unimorph. We can derive the capacitance energy while combining the piezoelectric equation and the stress in the cantilever together. The stiffness of electrode is ignored and it is assumed that electrodes cover the whole of piezoelectric layers. When a force W is applied, the piezoelectric energy can be expressed as:

$$U_{cor} = \frac{1}{2}\frac{\varepsilon\, b\,(1-2\gamma)(l_2 - l_1)}{t_c} \times \left[-\frac{1}{4}\frac{d_{31}W}{\varepsilon I}\left\{\left(\frac{d}{2}+t_c\right)^2 - \left(\frac{d}{2}\right)^2\right\}(l_2+l_1)\right]^2 \qquad (2)$$

where d_{31} is the piezoelectric property, ε is the dielectric constant, I is the moment of inertia. The piezoelectric energy of the corrugated beam is therefore a strong function of the distance d. The piezoelectric energy of unimorph can be expressed by Eq. 3 when young's modulus of base layer is assumed to be the same as of the piezoelectric layer:

$$U_{uni} = \frac{1}{2}\frac{\varepsilon\, b\,(l_2 - l_1)}{t_b}\left[-\frac{1}{4}\frac{d_{31}W}{\varepsilon I}t_b{}^2(l_2+l_1)\right]^2 \qquad (3)$$

Since we set the moment of inertia to be the same, the strain energy should be the same when the same force is applied. Therefore we can compare the energy conversion efficiency of the structure by means of comparing the piezoelectric energy. The normalized piezoelectric energy of corrugated beam is:

$$\frac{U_{cor}}{U_{uni}} = 2\alpha(\alpha+\beta)^2(1-2\gamma) \qquad (4)$$

Fig. 3 shows this normalized conversion efficiency of unimorph, bimorph, and corrugated structures with the same resonance frequency and under the same bending force. It is found that if β is chosen correctly, the corrugated beam energy harvester could achieve the same or higher energy conversion efficiency as the bimorph structure. The same trend was also verified by Finite Element Analysis.

FABRICATION PROCESS

Figure 4 shows the fabrication process flow for the corrugated beam energy harvester. The whole process is similar to the fabrication of the conventional unimorph energy harvester except the additional silicon groove etching step as the template for the

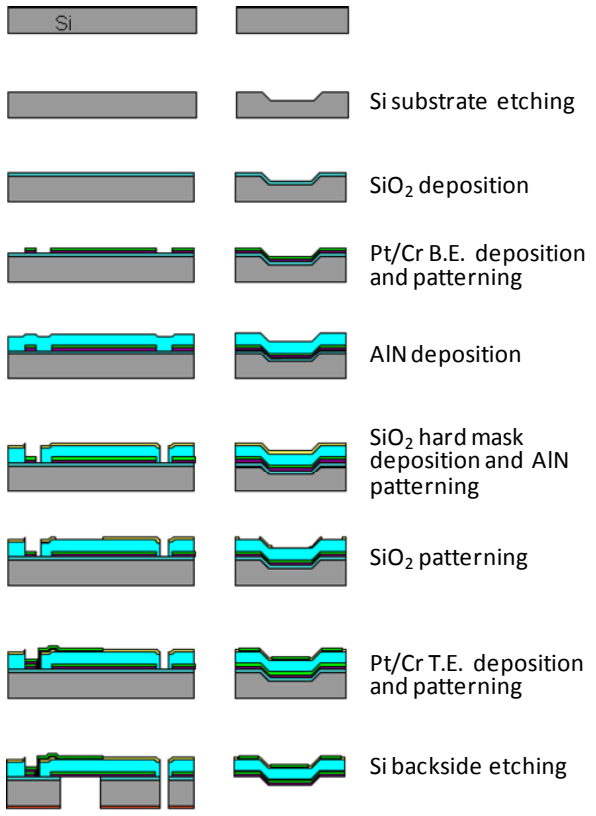

Fig. 4 Fabrication process of the corrugated beam energy harvester which starts with the etching of the substrate as a template for the corrugation design. Only a single AlN deposition is required.

corrugation design.

The groove was etched into 680μm-thick silicon wafer by RIE (Reactive Ion Etching), followed by a PECVD process (Plasma Enhanced Chemical Vapor Deposition) for 0.5μm-thick silicon oxide layer as an insulation as well as the stop layer for the backside etching process in a later step. Afterwards, a 0.1μm-thick Cr/Pt bottom electrode was deposited by sputtering and patterned by a lift-off process. Next, a 2μm-thick piezoelectric AlN layer was deposited on the bottom electrode by sputtering at 300°C and a 0.3μm-thick silicon oxide layer was deposited and patterned as a hard mask to etch AlN in 40°C TMAH. After the AlN etch process, this silicon oxide hard mask was patterned to form the through window for the top electrode. The top electrode made of Cr/Pt was deposited and patterned on the through window. Finally the proof mass was released by backside DRIE (Deep Reactive Ion Etching) silicon etching. Figure 5 shows an SEM image of the corrugated beam energy harvester.

MEASUREMENT AND DISCUSSION

Two types of electrical connections were designed and tested. The first one is the verification model (Fig. 6) where the bottom electrodes are divided to verify the directions of the generated electric fields above and below the neutral plane of the piezoelectric layer. The

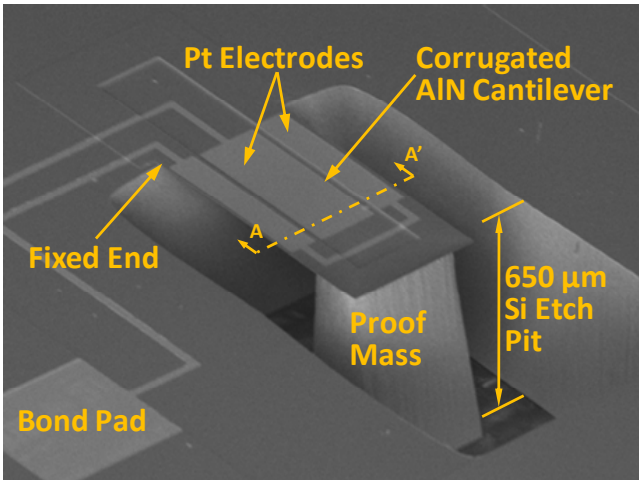

Fig. 5 SEM image of an AlN corrugated beam energy harvester.

second one is the practical model (Fig. 7) where the bottom electrodes are connected as a common potential to simplify the routing and to increase the output voltage in serial.

Figure 6 shows the output voltage from the verification model with a pulse input. The dimensions of the silicon proof mass are $b = 400\mu m$, $2l_1 = 500\mu m$, and $t = 680\mu m$. The dimensions of the corrugated beam are $b = 400\mu m$ and $l_2 = 250\mu m$ with the distance between upper and lower piezoelectric layers $d = 2.4\ \mu m$. In order to verify the polarity of electric fields at each part, Channel 1 and 3 are connected to the upper parts of the corrugated piezoelectric AlN layer while Channel 2 is connected to the lower part. Since AlN polarization is along [001], the symmetric voltage readout from upper and lower corrugated beam proved that the neutral plane locates at the middle of the corrugation as designed and opposite electric fields can be extracted out from each piezoelectric AlN area without the need of inactive base layer.

A practical device with the same proof mass and beam dimensions but $d = 4.68\mu m$ was then mounted on a vibration stage and the relationship between the output voltage and drive frequency was plotted in Fig. 7. The resonance frequency of this device was observed at 2.56kHz. When an input acceleration of 0.25G was applied, the amplitude of output voltage was recorded at 180mV at a load resistance 0.86 MΩ. Therefore, the calculated output power of this device is 4.14nW. The theoretical maximum output power P_m from vibration energy harvester can be expressed in Eq. 5[6]:

$$P_m = \frac{2MY_0^{\,2}\omega^3 Q}{\pi} \tag{5}$$

where M is the mass of the proof mass, Y_0 is the amplitude of the input vibration, ω is the angular velocity and Q is the quality factor. With Q of 378 obtained from Fig. 7, the theoretical maximum power is 28nW and the conversion efficiency of this device

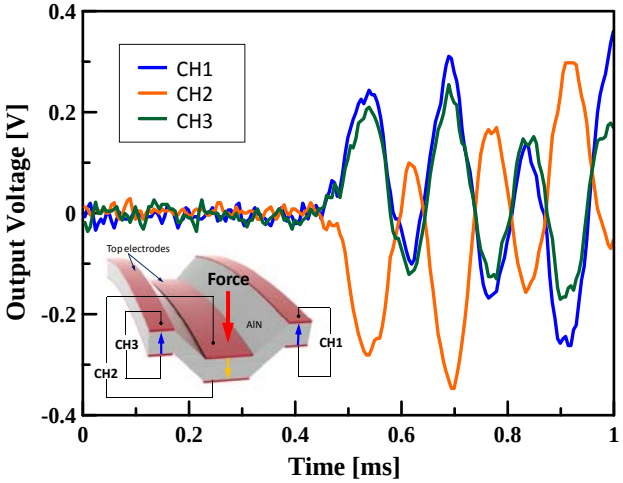

Fig. 6 Output voltages of proposed energy harvester under a pulse input where Channel 1 and 3 are connected to upper side and Channel 2 to lower side. Results validate the opposite direction of generated electrical potential.

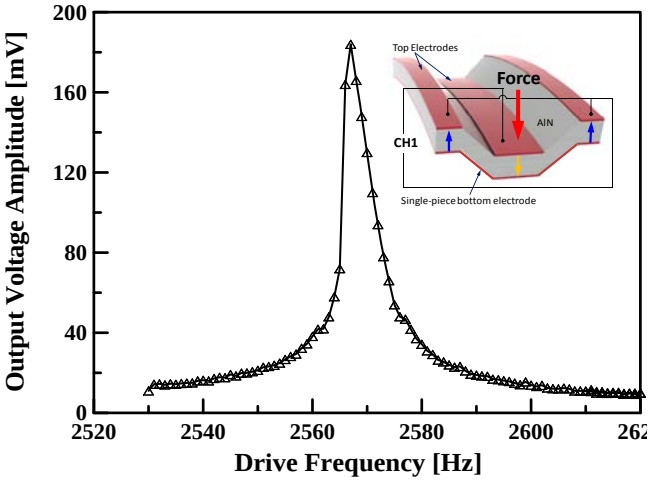

Fig. 7 Output voltage versus drive frequency measured from a practical design utilizing a single-piece bottom electrode.

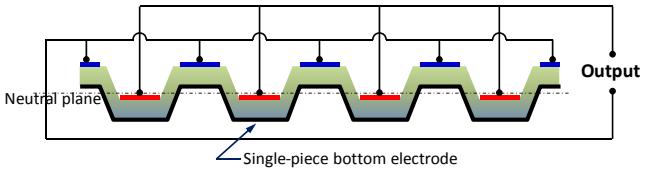

Fig. 8 A multi-fold design of corrugated cross-section beam with single-piece bottom electrode.

was calculated to be 15%.

It is worth pointing out that the distance d affects not only the conversion efficiency but also the resonance frequency of the energy harvester. Since the resonance frequency of the device is proportional to the square root of the moment of inertia, d is an important design parameter to determine the resonance frequency without changing other dimensions of the device. Devices with the same dimensions but $d = 2.4$ μm were also measured and the resonance frequency is 1.55kHz. The difference between the measured and predicted (1.15kHz) resonance frequencies is from the non-ideal connecting parts between upper and lower AlN layers and slanted sidewall of the proof mass.

Another advantage of the practical model is that the design can be connected in parallel to form a multi-fold corrugated cantilever as shown in Fig. 8. Such a multi-fold device with proof mass dimensions of b = 2400μm, $2l_1$ = 500μm, and t = 680μm, and the AlN corrugated beam dimensions of b = 2400μm, l_2 = 500 μm, and d = 4.68μm was recorded of 0.18μW output power under 1G acceleration. The resonance frequency was measured at 853Hz and the load resistance was 1.1MΩ.

CONCLUSION

The corrugated MEMS piezoelectric energy harvester has been designed and fabricated with experimental characterizations. The generated electric fields above and below the neutral plane have been verified to be opposite and could be extracted out individually. The distance d is an important design factor to maximize the conversion efficiency and to establish a specific resonance frequency without changing other parameters. As presented, this corrugated-cross-section piezoelectric structure combines advantages of simple fabrication process from unimorph design and high energy conversion efficiency from bimorph design and could find potential applications as MEMS piezoelectric energy harvesters.

REFERENCES

[1] S. Roundy et al., Improving power output for vibration-based energy scavengers, *IEEE Pervasive Computing*, vol. **4**, no. **1**(Jan.-Mar. 2005) 28–36

[2] M. Renaud et al., Fabrication, modeling and characterization of MEMS piezoelectric vibration harvesters, *Sensors and Actuators* A 145–146 (2008) 380–386

[3] H.-B. Fang et al., Fabrication and performance of MEMS-based piezoelectric power generator for vibration energy harvesting, *Microelectronics Journal* **37** (2006) 1280–1284

[4] D. Shen et al., The design, fabrication and evaluation of a MEMS PZT cantilever with an integrated Si proof mass for vibration energy harvesting, *J. Micromech. Microeng*. **18**(2008) 055017 (7pp)

[5] P. Muralt et al., Vibration energy harvesting with PZT micro device, *Procedia Chemistry* **1**(2009) 1191–1194

[6] P. D. Mitcheson et al., Performance limits of the three MEMS inertial energy generator transudation types, *J. Micromech. Microeng.* **17**(2007) S211–S216